Thermochimica Acta 511 (2010) 179–188

Contents lists available at ScienceDirect

Thermochimica Acta

journal homepage: www.elsevier.com/locate/tca

Composition optimization of PEEK/PEI blend using model-free kinetics analysis

R. Ramani, S. Alam*

Polymer Science Division, D.M.S.R.D.E., G.T. Road, Kanpur 208013, India

ARTICLE INFO

Article history:
Received 23 June 2010
Received in revised form 10 August 2010
Accepted 12 August 2010
Available online 19 August 2010

Keywords:
Poly(ether ether ketone)
Poly(ether imide)
Miscible blend
Thermal stability
Model-free kinetics
Activation energy

ABSTRACT

We report here the investigations on the thermal and thermo-oxidative degradation kinetics of a miscible high performance polymer blend poly(ether ether ketone)/poly(ether imide) (PEEK/PEI) with various compositions, measured in argon and air medium, respectively. The derivative thermogravimetric results indicate two-stage decomposition for both thermal and thermo-oxidative degradation for the entire composition of PEEK/PEI blend. Interestingly, the PEI addition is found to enhance the thermo-oxidation rate of PEEK. The effective activation energy (E_α) as a function of conversion (α) is found for both the processes using model-free kinetics. The model-free kinetics results reveal that the blend with 50% PEI content show high E_α value and the differential scanning calorimetry results corroboratively show a significant change in crystallinity for this PEI composition. Based on these results, the blend with composition 50/50 (PEEK/PEI) is suggested to have optimum thermal stability.

1. Introduction

Poly(ether ether ketone) (PEEK) is a high performance engineering semicrystalline thermoplastic having excellent chemical resistance and superior mechanical properties [1–5]. It is suitable for use as a matrix material in the preparation of thermoplastic composites owing to its good adhesion to glass and carbon fibres [6,7]. However, because of its relatively low glass transition temperature (T_g) of around 145 °C, the modulus of these materials decreases at elevated temperatures [5]. On the other hand, poly(ether imide) (PEI) is an amorphous polymer with comparatively high T_g of around 215 °C [5,6]. But, PEI has a lower chemical resistance than that of PEEK and cannot be used above its T_g [5,7]. Blending of these two polymers combines the complimentary properties of both of them and hence PEEK/PEI blends have been the subject of several investigations for more than two decades [2,4–17]. Now, it is a proven fact that PEEK and PEI are molecularly miscible in the amorphous state [2,4–7].

With the improved T_g, the PEEK/PEI blend is a suitable matrix resin in the preparation of high performance composites for aerospace applications as well as for conventional spare parts in aircraft components [17–19]. For this, good thermal and oxidation stability and retention of physical properties at high temperatures are required because they can be subjected to drastic thermal conditions in service or during repair [3,20,21]. Thus, degradation studies on PEEK/PEI blend in various environments and the associated kinetics are of paramount importance. The common method for determining the behavior such materials at high temperatures is by studying their thermal degradation at elevated temperatures using thermogravimetric analysis (TGA) [22]. Despite of many aspects that have been studied on PEEK/PEI blends [2,4–17], the thermal decomposition studies on PEEK and PEI using TGA are mostly directed in understanding its degradation temperature, and thereby to correlate with other physical and mechanical properties [17,23].

Temperature changes can stimulate a variety of chemical and physical processes in polymeric systems like thermal degradation, cross-linking, crystallization, glass transition, etc. [24]. Thus, the nature of the polymer degradation kinetics is complex as they include information about simultaneously occurring multiple steps. Results of the ICTAC kinetics project [25] suggested that isoconversional methods could provide a solution to this challenge. In the recent years, the model-free kinetics method, which is based on Vyazovkin's theory for the kinetics studies of complex reaction [26–28] has become a popular method in obtaining a reliable and consistent kinetic information on the thermal degradation process in many polymers and polymer composites [24,28–34]. In the model-free kinetics, the dependence of effective activation energy (E_α) on the degree of conversion (α) is found through which single-step or multi-step nature of the decomposition mechanism can be confirmed [33–35]. The model-free kinetics also enables

* Corresponding author. Tel.: +91 512 2451700; fax: +91 512 2450404.
E-mail address: sarfarazkazmi@yahoo.com (S. Alam).

0040-6031/$ – see front matter © 2010 Elsevier B.V. All rights reserved.
doi:10.1016/j.tca.2010.08.012

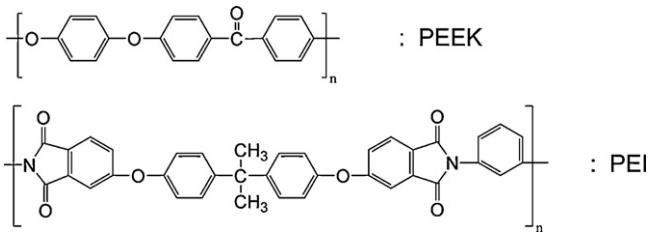

Scheme 1. Chemical formulas of PEEK and PEI.

the prediction of reaction kinetics over a wide temperature range [28,29,33,34].

Furthermore, the variation of E_α as a function of α is considered as one of the important parameters to understand the thermal stability of the polymers [35,36]. A polymer with higher E_α value is expected to be more stable [35,36]. The E_α value of the blend can be higher or lower than that of both the individual polymers from which it was obtained [37–39] or to one of them [34,40,41]. Incorporation of nanomaterials to polymers has shown to increase the E_α value of the resulting polymer nano-composites [28,35,36].

Nevertheless, to the best of our knowledge, there are no scientific works to date that employs model-free kinetics analysis to understand the thermal stability of PEEK/PEI blends. Scientific curiosity has thus stimulated us to investigate whether PEEK/PEI blend could be optimized based on model-free kinetics. In the present study, using the model-free kinetics [26–28], we provide the effective activation energy (E_α), the conversion rates and the degradation time as a function of temperature for the thermal and thermo-oxidative degradation for various compositions of PEEK/PEI blend and thereby suggest the optimum blend composition. The differential scanning calorimetry (DSC) results corroborate the model-free kinetics data.

2. Experimental

2.1. Sample preparation

Granular PEEK-grade Victrex 450G was purchased from Victrex, U.K. and the PEI-grade Ultem 1000 was obtained from General Electric Plastics, Europe. Both PEEK and PEI were used as received and were dried for 48 h at 120 °C under vacuum. Blending was performed on a corotating twin-screw extruder at ca. 370 °C. The strand leaving the extruder was quenched in a water bath, air dried and chopped in to granulates. Blends with weight ratios of PEEK/PEI 100/0, 90/10, 80/20, 70/30, 50/50, 30/70 and 0/100 were prepared. These blends are designated, respectively as P_0, P_{10}, P_{20}, P_{30}, P_{50}, P_{70} and P_{100} (where the subscripts represent the wt% of PEI). The blends were subsequently injection molded at ca. 380 °C in to square plates (60 mm × 60 mm × 3 mm). The chemical structure of the PEEK and PEI is shown in Scheme 1.

2.2. Characterization

Although the main aim of the work is to understand the thermal decomposition kinetics of PEEK/PEI using model-free kinetics as applied to its TGA results, we have first performed differential scanning calorimetry (DSC) measurements to identify the glass transition temperature (T_g) of the various proportions of this blend and thereby to make sure that the blend used in the present investigation is miscible. The T_g has been taken as the inflexion temperature of the heat flow, the peak temperature of the endothermic heat flow as melting temperature (T_m) and the peak temperature of the exothermic heat flow (during cooling) as the crystallization temperature (T_c). For DSC experiment, DSC Q200 (TA instruments) was employed. The instrument was calibrated using indium standard. Samples of ~6 mg were weighed and sealed in aluminum sample pans and were heated above their melting temperature for 5 min and then cooled to erase the thermal history. Then the samples were reheated with a heating rate of 20 °C/min and the T_g and T_m were taken from the second heating traces and T_c from the corresponding cooling traces.

Thermogravimetric analysis was performed using a TGA (Mettler-Toledo TGA/SDTA 851^e) instrument in the temperature range 30 to 1100 °C. The instrument was calibrated using a Mettler-Toledo total calibration procedure with respect to the indium and aluminum standards. Samples (~6 mg) for TGA measurements were placed in 70 μL alumina crucibles. The buoyancy effect in TGA has been accounted for by performing empty pan runs and subtracting the resulting data from the subsequent sample mass loss data. Thermal decomposition experiments were carried out in dynamic conditions using the nominal heating rates of 5, 10, 15 and 20 °C/min both in argon and dry air atmosphere (flow rate in each case was maintained at 50 mL/min). In the temperature program, an initial 10 min isothermal segment allowed the furnace to purge with argon/dry air and then the temperature was ramped to 1100 °C at the specified heating rate. The T_{onset} is the onset temperature corresponding to the start of degradation (the intersection of the extrapolated base lines with tangents drawn in the inflection points of the TG curve), T_{max} is the temperature at the maximum rate of degradation and R_{900} is the percentage residue at 900 °C. Mettler-Toledo STAR^e software (ver 9.0) was used to perform the model-free kinetics calculations that provide activation energy as a function of extent of conversion. This software also helps for lifetime predictions of the measured sample.

2.3. Model-free kinetics (MFK)

The rate of a thermal reaction depends on the extent of conversion (α), temperature (T) and time (t). Here, the degree of conversion (α) is defined as the ratio $(m_i - m)/(m_i - m_f)$ where m_i, m and m_f refer to the initial, actual and final mass of the sample. For each process, the reaction rate as a function of conversion, $f(\alpha)$ is different and must be determined from the experimental data. The dependence of α on temperature is customarily expressed as

$$\frac{d\alpha}{dt} = k(T) f(\alpha) \quad (1)$$

where $k(T)$ is the rate constant and $f(\alpha)$ is the reaction model [27]. Depending on the reaction mechanism, the reaction model may take various forms. The temperature dependence of the rate constant is expressed in terms of Arrhenius equation as

$$k(T) = A \exp\left(\frac{-E}{RT}\right) \quad (2)$$

where T is the temperature, R is the gas constant, A is the pre-exponential factor and E is the activation energy.

Substitution of Eq. (2) to Eq. (1) yields

$$\frac{d\alpha}{dt} = A \exp\left(\frac{-E}{RT}\right) f(\alpha) \quad (3)$$

As mentioned earlier, the degradation of polymers tends to demonstrate complex kinetics that cannot be described by Eq. (3) alone throughout the whole temperature region [28,35]. The model-free kinetics method is based on the realization that the activation energy indeed depends on the extent of conversion (α) but they are always same at a particular conversion independent of the heating rate used. Thus, model-free kinetics (MFK) method is also called as an isoconversional method [28]. The isoconversional methods may be best known through their most popular representatives, the methods of Friedman [42], Ozawa [43] and Flynn and

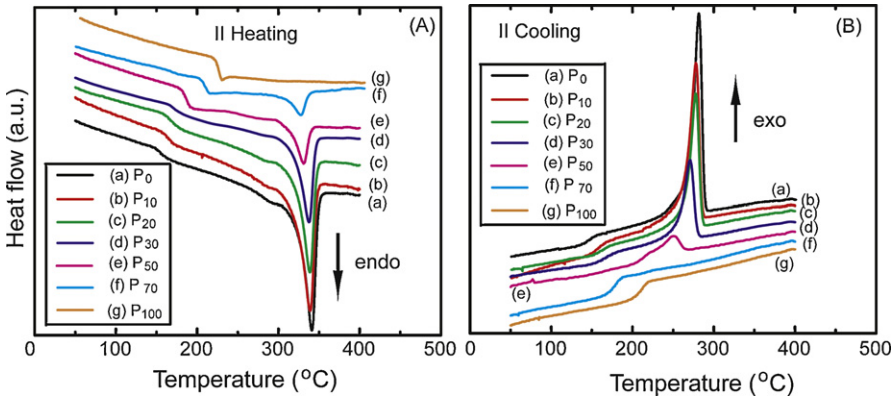

Fig. 1. The DSC plots for different ratios of PEEK/PEI upon second heating (A) and cooling (B).

Wall [44]. The model-free kinetics is a computer programmer based on Vyazovkin's theory for the kinetics studies of complex reaction [26–28]. Applying the model-free kinetics, accurate evaluations of complex reactions can be performed in order to obtain reliable and consistent kinetic information about the overall process. The data analysis in this approach follows all the points of conversion from multiple experiments. The main features of this method are given in the following paragraph and more details can be found in a recent review [28].

According to model-free kinetics method [26–29], for a given extent of conversion, the reaction rate is only a function of temperature.

$$\left[\frac{\mathrm{d}\ln(\mathrm{d}\alpha/\mathrm{d}t)}{\mathrm{d}T^{-1}}\right]_{\alpha} = \frac{-E_{\alpha}}{R} \tag{4}$$

The isoconversional rates in Eq. (4) are determined as the rates to reach a given extent of conversion in several runs performed at different heating programs. The isoconversional method assumes that E_α is constant only at a given extent of conversion and the narrow temperature region related to this conversion at different heating rates [35]. The thermal degradation is carried out at least in three different heating rates (β) and the respective conversion curves are calculated from the measured TG data. For each conversion (α), $\ln(\beta/T^2)$ is plotted against $1/T_\alpha$ that results to a straight line with slope ($-E_\alpha/R$), thus providing the E_α as a function of α [24,27,28,33]. This plot enables to explore lifetime prediction of the polymer under study and the mechanisms of the thermally stimulated processes.

3. Results and discussion

First we discuss on the miscibility aspect of this PEEK/PEI blend from the DSC measurements. Listed in Table 1 are the T_g, T_m, T_c, the enthalpy of melting (ΔH_m) and the enthalpy of crystallization (ΔH_c) of the PEEK/PEI blends from the second DSC traces. The second heating and cooling DSC curves are shown in Fig. 1A and B, respectively. The T_g values obtained for various blend compositions

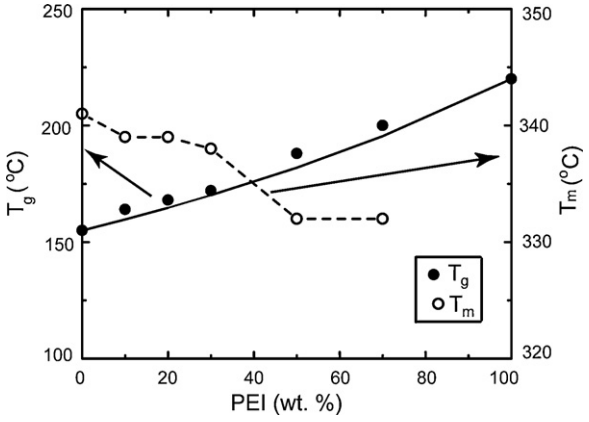

Fig. 2. The variation of T_g and T_m of PEEK/PEI blends vs. PEI composition from the second DSC heating scans at 20 °C/min. The solid line represents the Fox equation.

are comparable to the reported values for the similar grade of PEEK and PEI [6,10,23]. All the samples showed T_g, T_m during heating and T_c during cooling (except P_{70} and P_{100}). The blends showed single T_g in the entire blend composition and the values of T_g of these blends increased with the increasing PEI content. Fig. 2 shows the plot of T_g and T_m values of the blends against PEI composition. The solid line represents the fit from well-known Fox equation:

$$\frac{1}{T_g} = \frac{w_1}{T_{g1}} + \frac{w_2}{T_{g2}} \tag{5}$$

where w_1 and w_2 represent the weight fractions of the blend constituents, and T_{g1} and T_{g2}, their respective glass transition temperatures. The single T_g obtained for the entire blend composition approximately obeyed the Fox equation within experimental error (Fig. 2). These results suggests that the PEEK/PEI blends used in the present study are indeed miscible as reported [2,5,6].

When amorphous PEI is added to semicrystalline PEEK and upon crystallization of the latter, PEI is rejected into the amorphous domains of PEEK. Hence, there is a progressive enrichment of PEI in

Table 1
DSC results of PEEK/PEI blends during 2nd heating and cooling at 20 °C/min.

PEEK/PEI	T_g (°C)	T_m (°C)	ΔH_m (J/g)	T_c (°C)	ΔH_c (J/g)	χ_c (wt%)	$\chi_{c(PEEK)}$ (wt%)
100/0	155	341	31.9	282	37.3	24.5	24.5
90/10	164	339	27.9	278	32.7	21.5	23.9
80/20	168	339	25.8	277	30.9	19.9	24.9
70/30	172	338	21.4	271	20.6	16.5	23.6
50/50	188	332	5.2	248	7.3	4.0	8.0
30/70	200	332	1.9	–	–	1.5	5.0
0/100	220	–	–	–	–		

Table 2
Non-isothermal TGA experimental results for PEEK/PEI blend.

Sample	Argon medium				Air medium			
	β (°C/min)	T_{onset} (°C)	T_{max} (°C)	R_{900} (%)	T_{onset} (°C)	T_{max1} (°C)	T_{max2} (°C)	R_{900} (%)
P_0	5	532	568	49.7	549	567	617	0.4
	10	553	585	50.6	552	570	**	1.1
	15	571	597	52.4	555	578	**	1.9
	20	576	599	53.5	559	583	**	3.2
P_{10}	5	519	549	53.1	529	562	583	0.3
	10	531	564	54.3	550	569	639	1.5
	15	552	579	53.9	555	575	**	2.0
	20	555	583	56.0	560	578	**	4.9
P_{20}	5	513	540	48.0	518	543	615	0.3
	10	530	561	50.5	535	557	624	2.5
	15	547	570	52.8	545	565	679	2.2
	20	550	578	51.6	553	576	690	3.0
P_{30}	5	510	531	53.2	515	534	633	0.4
	10	526	552	52.4	532	551	645	1.1
	15	537	560	54.5	542	562	667	1.6
	20	540	565	54.2	551	569	717	1.5
P_{50}	5	504	550	46.2	512	554	617	1.2
	10	520	558	46.0	530	566	640	1.6
	15	523	571	45.9	536	573	664	2.8
	20	534	574	45.4	541	583	671	1.7
P_{70}	5	504	525	56.0	499	520	602	2.7
	10	521	542	55.7	512	540	639	3.4
	15	524	550	54.5	522	550	658	2.8
	20	533	556	53.8	534	558	711	2.5
P_{100}	5	498	521	50.6	510	527	602	0.4
	10	510	540	55.7	526	541	629	1.6
	15	529	550	53.7	529	548	649	1.2
	20	533	556	52.6	535	557	672	2.5

T_{onset} = onset degradation temperature; T_{max} = maximum degradation temperature; R_{900} = residue at 900 °C; β = heating rate; ** = no identifiable derivative maximum.

the amorphous regions of PEEK [15]. This leads to a change in the composition of the amorphous phase of PEEK. Thus, the increase in T_g of the blend with increase in PEI composition implies increase of mobility restrictions brought to the amorphous segments of PEEK. The T_m which showed a slight decrease with increase in PEI content, decreased significantly when the PEI content in the blend reaches 50% (Figs. 1A and 2). The absence of T_c and the associated ΔH_c for P_{70} blend shows there is no appreciable crystallization at this high PEI content (see Fig. 1B and Table 1). Although the values of ΔH_m and ΔH_c show a gradual decrease with increase in PEI content, due to the hindrance to PEEK crystallization posed by amorphous PEI segments [5], their values change significantly when PEI content in the blend is ≥50% (see Table 1). This reveals greater extent of perturbation to PEEK crystallization by PEI matrix, when the composition of PEI in the blend is ≥50%.

There are three possible morphologies suggested for polymer blends obtained from semicrystalline/amorphous combination depending on the location of the amorphous domain in the semicrystalline matrix; interlamellar, interfibrillar and interspherulitic [9]. If a complete rejection of PEI from the PEEK crystalline interlamellar zones occurs, the reorganization of PEEK crystals in the blend should be identical to that of pure PEEK [8,15]. On the other hand, if PEI is contained in the interlamellar regions, the PEEK crystal reorganization should be changed [8], which in turn, will reflect on its melting temperature (T_m). Interestingly, in our case, significant decrease in melting temperature is seen only when PEI content in the blend is ≥50% indicating possible interlamellar segregation of PEI [8] at this composition onwards. Furthermore, in case of miscible blends, it is known that the melting temperature of the crystallizable component usually gets depressed by the strong segmental interaction [9].

To further understand the influence of PEI on PEEK crystallinity, the levels of crystallinity (χ_c) and its normalized value ($\chi_{c(PEEK)}$) by the PEEK weight fraction (W_{PEEK}) in the blend are estimated from the DSC results [5] using the equation:

$$\chi_c = \frac{\Delta H_m}{\Delta H^\circ_m} \quad (6)$$

$$\chi_{c(PEEK)} = \frac{\chi_c}{W_{PEEK}} \quad (7)$$

where ΔH°_m is the extrapolated value of the enthalpy corresponding to the melting of a 100% crystalline PEEK sample, taken as 130 J/g [6,17]. Both the χ_c and $\chi_{c(PEEK)}$ values show a significant decrease when the PEI content in the blend is ≥50% (see Table 1). Thus, PEI weakly influences the crystallization of PEEK in PEEK/PEI blend when the PEI content is <50% and exhibit a significant decrease when the PEI content in the blend is ≥50%.

Thermogravimetry is the most widely used technique to characterize the thermal decomposition of polymers. Fig. 3(A–D) shows the typical TG curves of normalized mass and derivative thermogravimetry (DTG) data of the derivative mass of PEEK (sample P_o) taken at four different heating rates 5, 10, 15, and 20 °C/min in argon and air media. The TGA results of onset temperature (T_{onset}), the maximum degradation temperature (T_{max}) and the residue at 900 °C (R_{900}) for the entire blend composition at the four different heating rates in argon and air media are tabulated in Table 2. The T_{onset} of PEEK increases with increase in heating rate both in argon and air media (Table 2) similar to the results reported in many polymers [33,45].

From the DTG plots (Fig. 3C and D), it is evident that PEEK undergoes two-step degradation both in argon and air medium, in accordance with previous studies [46,47]. However, the DTG plot

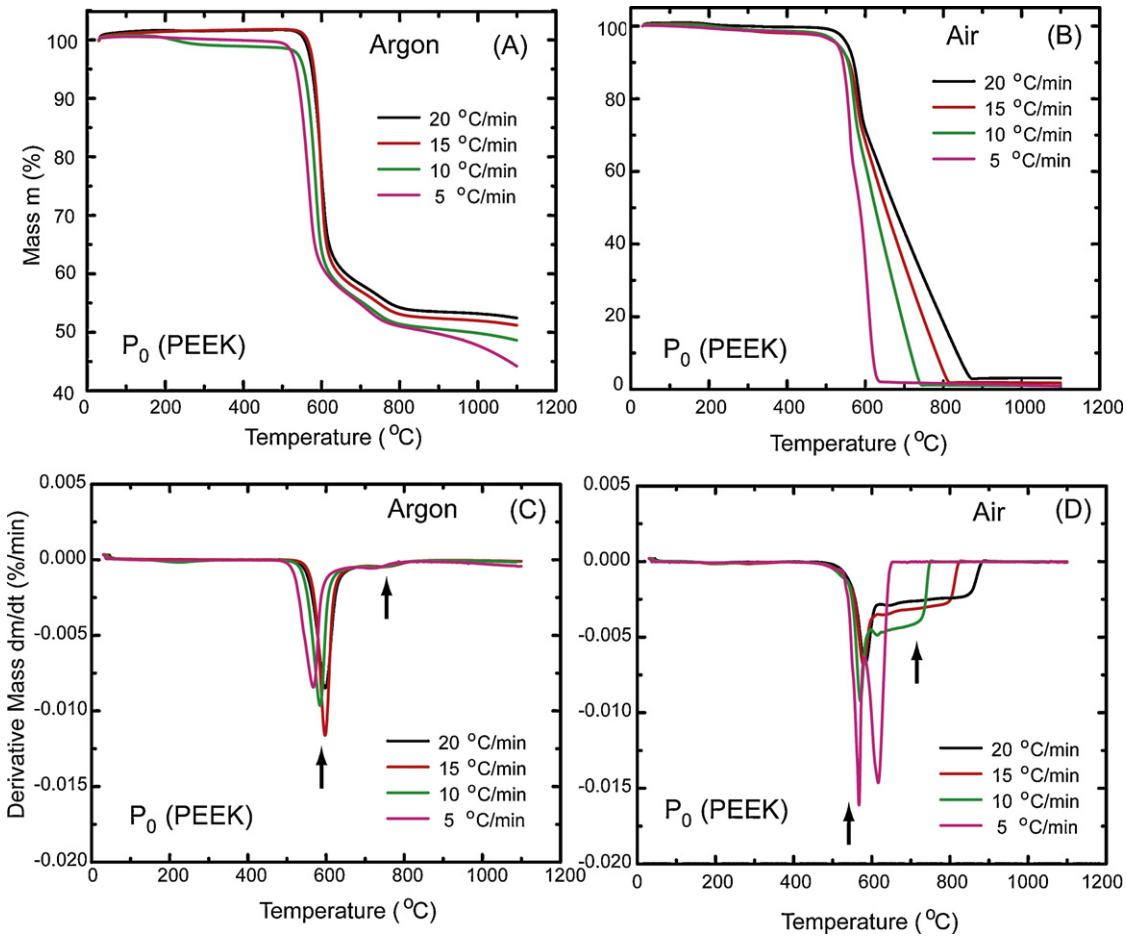

Fig. 3. Typical thermograms of PEEK with four different heating rates in argon medium (A) and air medium (B). Their DTG curves in argon medium (C) and air medium (D).

of PEEK in air medium (Fig. 3D), shows an interesting change at the second degradation step, that its rate of degradation increases with decrease in heating rate. This second degradation in PEEK is due to thermo-oxidation [46,47]. At higher heating rates, oxygen diffusion rate is too slow in comparison to the heating rate and temperature rise [47]. The lower heating rate permits greater diffusion of oxygen through the melt and thereby the rate of thermo-oxidation gets enhanced. We will discuss this result in more detail later, in the context of influence of PEI on the thermo-oxidation of PEEK.

Fig. 4(A–D) depicts the typical TG curves of normalized mass and DTG data of the derivative mass for various composition of PEEK/PEI at a heating rate of 20 °C/min in argon medium. The corresponding plots in air medium are given in Fig. 5(A–D). As observed in PEEK, the DTG thermograms illuminate two-step decomposition process in PEEK/PEI blend both in argon and in air medium. From Figs. 4(A–D) and 5(A–D), it is evident that the thermal degradation curves of PEEK/PEI in argon and in air media coincide up to ca. 480 °C and differ beyond this temperature, which leads us to assume that oxidation mechanisms occur during the later part of the degradation. The DTG curves in these figures makes clear that the rate of second degradation step is mild in argon medium whilst it is prominent in air medium and comparable to their first degradation rate when the PEI content is >10%. During the final phase of degradation, mass loss incurred is less in argon medium leading to a thermostable residue (45–56%), while in air medium, the dominant oxidation leads to a negligible residue (0.3–4.9%). This indicates that PEEK/PEI blend is very sensitive to the presence of oxygen.

In case of PEEK (Fig. 4A; sample P_0), with a heating rate of 20 °C/min, the first degradation step in argon medium begins at ca. 576 °C with the T_{max} at 599 °C. The second degradation is mild and occurs between ca. 710 and 850 °C. The residue at 900 °C (R_{900}) is 53.5% and results to highly flame retardant material because of its high carbonization structure. Unlike in argon medium, both the degradation steps are prominent in air medium (Fig. 5A). The first degradation step in air commences at 559 °C and ends at ca. 620 °C with T_{max1} at 583 °C and has a decomposition product of ca. 82%. The first degradation is followed immediately by another significant degradation step (between ca. 620 and 890 °C) with no identifiable peak maximum. This process leads to a negligible residue (<4%).

Similar to PEEK, PEI (Fig. 4B; sample P_{100}) also shows two distinct degradation steps in argon and air and is in accordance with the earlier reports [20]. At a heating rate of 20 °C/min in argon medium, the first degradation starts at ca. 533 °C with T_{max} at 556 °C while the second degradation step starts instantly after the first degradation with no prominent maximum and a residue of ca. 53% at 900 °C due to carbonization. In air medium, the first step commences at ca. 535 °C with T_{max1} at 557 °C and ends at ca. 585 °C (Fig. 5B). The second degradation (between ca. 585 and 780 °C) has T_{max2} at 672 °C with residue at 900 °C to be <3%. The TGA results of PEEK and PEI given in Table 2 are comparable to their reported values [20,46–49].

The TGA results of various compositions of PEEK/PEI blend studied mostly lie between the values reported for PEEK and PEI discussed above by showing two-step degradation both in argon and air medium. As mentioned earlier, only at the later stages of degra-

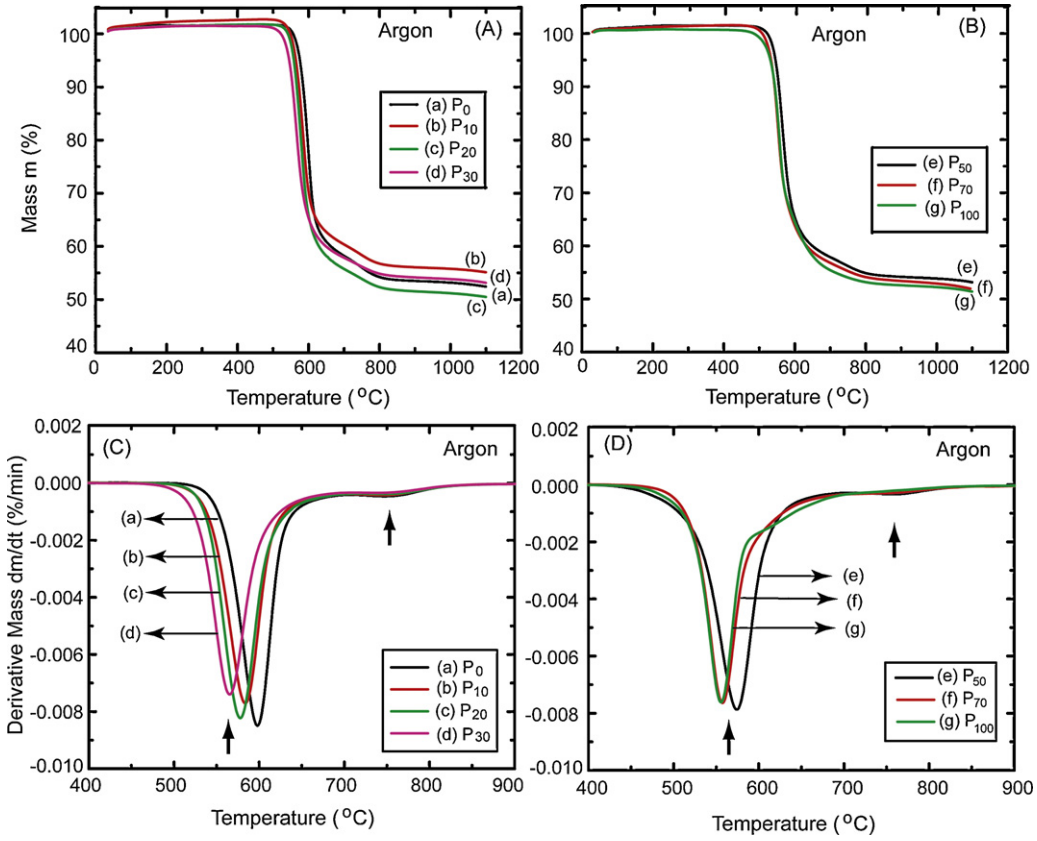

Fig. 4. Typical thermograms for different ratios of PEEK/PEI with the heating rate 20 °C/min in argon medium (A and B). Their corresponding DTG curves (C and D).

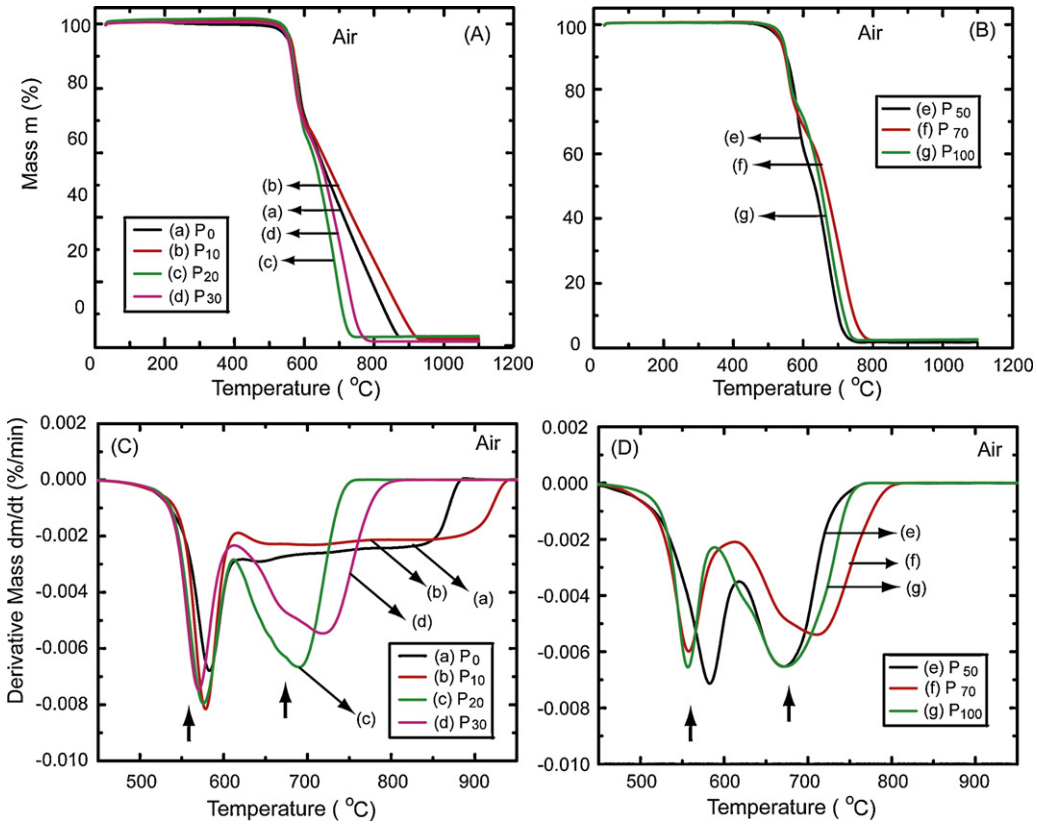

Fig. 5. Typical thermograms for different ratios of PEEK/PEI with the heating rate 20 °C/min in air medium (A and B). Their corresponding DTG curves (C and D).

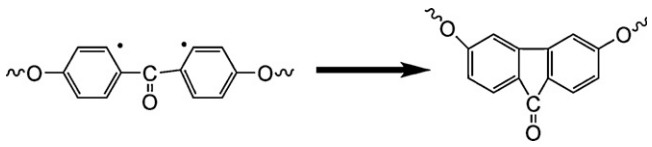

Scheme 2. Fluorenone structure formation due to cyclization of diradicals.

dation (above ca. 480 °C), the thermal stability of PEEK/PEI blend is strongly influenced by the type of atmosphere. Except when the PEI composition is ≤10% (samples P_0 and P_{10}), both the decomposition steps are prominent in air medium. Another interesting aspect that could be observed from the DTG plots in air medium (Fig. 5C and D) is that the width of the first degradation peaks are almost the same for the entire blend composition while the width of the second degradation peaks narrows with PEI content. But, no significant change in width of the degradation peaks could be seen in argon medium (Fig. 4C and D).

Now, let us analyze the mechanism of the degradation of the blends and the probable end products after degradation. To understand the decomposition of PEEK/PEI blends, we bring here the analogy from the pyrolysis studies reported for both PEEK and PEI [20,46,47]. In a study on the pyrolysis of PEEK by TGA/MS in an inert atmosphere [46], that was later confirmed by TG/FTIR [47], the authors observed the first major pyrolysis step at ca. 575 °C that was attributed to the main chain-scission of the ether and ketonic groups (see Scheme 1). The cleavage of the ether and ketonic groups mainly yielded phenol and CO_2, respectively. It has further been proposed that during the first pyrolysis step, a stable fluorenone structure was formed due to the cyclization of the adjacent diradicals in the ketonic group as shown in Scheme 2. The second step pyrolysis was mild and observed at ca. 800 °C due to cleavage of ketone group of the fluorenone structure formed in the first step [46,47]. This second step pyrolysis yielded CO_2 as the main pyrolysate [46,47].

In air medium, the first pyrolysis stage of PEEK was observed at ca. 570 °C due to random main chain-scission and carbonization mechanisms with a fluorenone structure formation [47]. This first step cracking resulted to CO and CO_2 as the major products with a small amount of phenol. In the second stage of pyrolysis that occurs at ca. 645 °C, the carbonized solid residue rapidly oxidized exclusively to CO and CO_2 [47].

In a pyrolysis study on PEI by TGA/MS in an inert atmosphere [20], the authors report the scission of the imide group (see Scheme 1) apparently plays an important role in two-stage pyrolysis process. The main pyrogram around 540 °C (first step) was due to CO_2 and the other dominant pyrolysates are phenol, benzene and aniline [20]. The partially carbonized structure undergoes further pyrolysis as second step above 560 °C with the remaining imide group formed to give CO_2 as the major product along with benzene and benzonitrile as pyrolysates [20].

Our results are in agreement with the two-step decomposition process discussed above for PEEK [46,47] and PEI [20]. We offer a similar explanation for the two-step decomposition observed in the blends and the expected end products could be a combination of what has been reported for PEEK and PEI depending on their composition in the blend. In order to explore the information about the thermal stability of the blends, the T_{max} (of first degradation step) obtained from the four different heating rates in argon and air medium as a function of PEI composition is plotted and are shown in Fig. 6A and B, respectively.

It is obvious that the T_{max} value depend on the composition of PEI in the blend. The value of T_{max} decreases with increasing PEI content up to 30%. Interestingly, for the blend P_{50}, the T_{max} value becomes high and is almost comparable to that of neat PEEK in air medium at all the four heating rates studied (Fig. 6B). Even in argon medium also, the P_{50} sample shows higher T_{max} value reflecting better thermal stability (Fig. 6A).

We now turn our attention towards the interesting changes in second degradation step. As stated earlier, in argon medium, the second degradation step is very mild and shows no significant change with PEI content in the blend (Fig. 4A–D). However, in air medium, the second degradation step becomes narrow with the increase in PEI content. This implies that the thermo-oxidation rate of PEEK is enhanced upon PEI addition (Fig. 5A–D). The diffusion of oxygen through the polymer melt controls the thermo-oxidation [47]. It is well known that in a semicrystalline polymer, the crystalline regions puts stiffer resistance for the diffusing species and the diffusion occurs through amorphous regions [50]. With the addition of PEI, the amorphous parts of the resultant blend increases which permit the diffusion of oxygen to a greater extent. This increased oxygen diffusion in turn facilitates its interaction to a greater extent with the polymer chains and thus enhances the thermo-oxidation rate.

The thermal degradation of polymers usually involves multiple steps characterized by different activation energy values. The relative contribution of these steps to the overall degradation rate changes with both temperature and extent of conversion. This means that the effective activation energy (E_α) determined from TGA data should be a function of these two variables. The dependence of E_α on the extent of conversion for the thermal degradation process of PEEK/PEI in

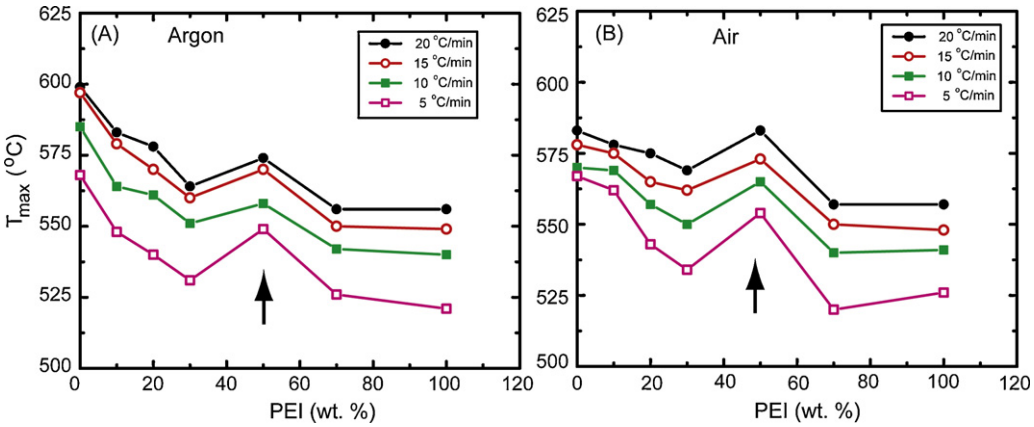

Fig. 6. Variation of maximum decomposition temperature (T_{max}) with PEI content in the PEEK/PEI blend at four different heating rates in argon medium (A) and in air medium (B).

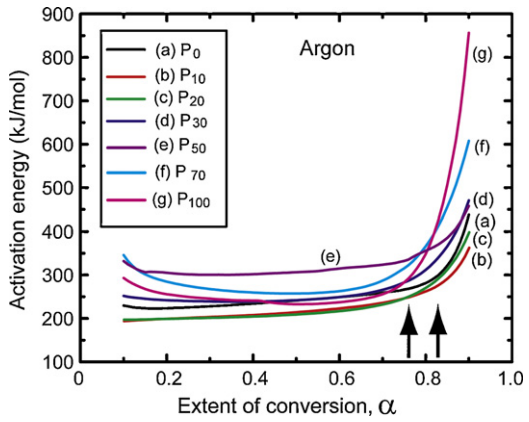

Fig. 7. The dependence of effective activation energy (E_α) on the extent of conversion (α) for the degradation of PEEK/PEI in argon medium obtained using model-free kinetics of TGA data.

argon medium is shown in Fig. 7 and that in air medium in Fig. 8.

In argon medium, PEEK has E_α value of ca. 233 kJ/mol at $\alpha = 0.1$ and exhibits a mild increase with conversion (Fig. 7). When $\alpha > 0.82$, the E_α value changes slope and shoot up to a value of ca. 441 kJ/mol at $\alpha = 0.9$. In comparison with PEEK, PEI has higher E_α value but the variation of E_α with α is similar to PEEK. For PEI, at the initial conversion level ($\alpha = 0.1$) E_α value is ca. 283 kJ/mol and remains almost unchanged up to $\alpha = 0.78$ and then rises sharply to reach ca. 848 kJ/mol at $\alpha = 0.9$. These two different trends of change in E_α values for PEEK and PEI in argon medium indicates their two-step decomposition pattern (see Fig. 4A–D). Comparison of change of slope in the variation of E_α vs. α for PEEK and PEI reveals that the second degradation step in PEI starts at a lower conversion level than PEEK (see Fig. 7). Even the DTG curves showed a similar trend (Fig. 4C and D).

The reported E_α value of PEEK in inert medium for first and second reaction regions are ca. 230 and 385 kJ/mol [46], and that for PEI is 230 and 406 kJ/mol [20]. It is evident from these numerical values that the obtained E_α values in the present study for the two reaction regions are comparable to the reported values. However, it is to be noted that the reported E_α values [46,20] are the average values for the particular reaction regions that covers a range of conversion and not for a particular conversion value. The change of E_α against α for the entire blend composition in argon medium follows a similar pattern to that of PEEK and PEI. But the value of E_α in the first reaction region remains relatively high for the blends with PEI content ≥50%.

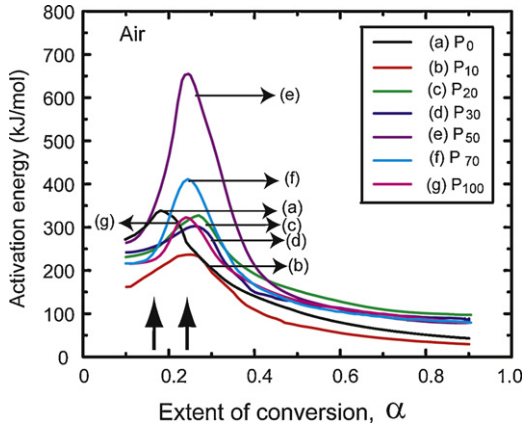

Fig. 8. The dependence of effective activation energy (E_α) on the extent of conversion (α) for the degradation of PEEK/PEI in air medium obtained using model-free kinetics of TGA data.

The variation of E_α vs. α in air medium for the blends is different, but quite interesting (Fig. 8). The E_α rises gradually in the beginning of conversion, peaks to a maximum and decreases almost exponentially. This dual trend in the E_α variation with α is in accordance with the two-step degradation exhibited by blends upon thermal-oxidation. The pure PEEK has E_α value of ca. 287 kJ/mol at $\alpha = 0.1$, attains a peak value of 338 kJ/mol at $\alpha = 0.17$ and thereafter decreases in a near exponential manner to reach a value of ca. 43 kJ/mol at $\alpha = 0.9$. The reported average E_α values for PEEK in air medium in the first reaction region is 230 kJ/mol and in the second reaction region is 159 kJ/mol [47]. In case of PEI, the E_α value is ca. 265 kJ/mol at $\alpha = 0.1$, attains a peak value of ca. 657 kJ/mol at $\alpha = 0.24$ and then decreases to ca. 89 kJ/mol when $\alpha = 0.9$.

For different composition of PEEK/PEI blends in air, the E_α value at the initial stages of conversion ($\alpha = 0.1$), do not exceed the values of their pure counterparts. Even, the peak values of E_α for the blends also lie below the value of PEEK and PEI when the PEI content is <50%. Surprisingly, the peak E_α value shows almost a two-fold increase compared to neat PEEK and PEI for P_{50} and remains relatively high also for P_{70} (Fig. 8). A polymer with higher E_α value is expected to have improved thermal stability [36]. In case of polypropylene/low density polyethylene (PP/LDPE) mixture, the authors found that the proportion of PP/LDPE that showed minimum E_α value also showed minimum T_{max} value [34]. In the present case, the sample P_{50} having exhibited high E_α value also exhibits high T_{max} value at all the four heating rates studied (Fig. 6B).

It is to be recalled here that the DSC measurements showed a significant decrease in crystallinity for the blend when the PEI content is ≥50% suggesting a possible interlamellar segregation of PEI chains. To activate the oxidation process in such an environment, the oxygen needs to mobilize in a torturous path through the lamellar bundles to reach the amorphous PEI segments. Hence the activation energy needs to be more for the sample P_{50}. In the case of P_{70}, since the crystallinity of the sample is negligible (Table 1), the E_α value is less compared to P_{50} (Fig. 8).

The decrease of E_α in PEEK is attributed to the initiation of the thermo-oxidation [47]. The E_α vs. α plot reveals that thermo-oxidation of pure PEEK gets initiated at $\alpha = 0.17$ and for pure PEI it is at $\alpha = 0.24$. As discussed earlier, the thermo-oxidation in PEEK commences at ca. 620 °C. From the TGA and DTG plots in air medium (Fig. 5A and C), $\alpha = 0.17$ in PEEK corresponds to a temperature of ca. 580 °C which is 40 °C less than the initiation temperature for thermo-oxidation. In case of PEI, $\alpha = 0.24$ corresponds to a temperature of ca. 585 °C which is the same as the initiation temperature for thermo-oxidation (Fig. 5B and D). Even in a recent thermo-oxidation study on poly(3-hexyl thiophene), we obtained a comparable value of thermo-oxidation initiation temperature in terms of mass change from TGA plot and E_α maximum from model-free kinetics [33].

These results indicate that the thermo-oxidation of PEEK begins earlier than what has been observed in TGA plot in terms of mass change. In fact, it has been reported that at fast heating rates, the first degradation step of PEEK can have contribution from both pyrolytic kinetics and oxidation degradation kinetics [47]. The possible reason suggested for this difference could be the stabilization of first stage decomposition by the rapidly formed fluorenone structure [47]. Thus, the model-free kinetics results seem to help to clearly identify the temperature at which the thermo-oxidation gets initiated in PEEK. However, more experiments are in progress using mass spectroscopy (MS) to identify the temperature at which the various gases evolve and to arrive at a conclusion in this regard.

From the TGA results, we know that the thermo-oxidation rate of PEEK gets enhanced upon PEI addition. In order to prove this aspect further, we have used model-free kinetics analysis results.

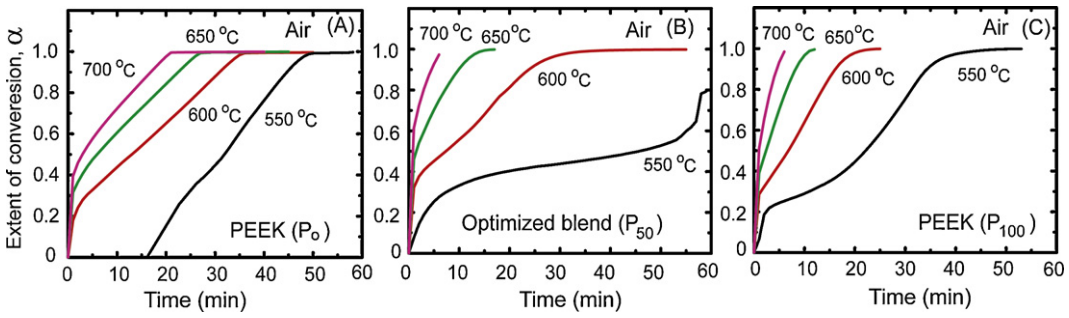

Fig. 9. Extent of conversion of PEEK (P_0; A), optimized PEEK/PEI (50/50) blend (P_{50}; B) and PEI (P_{100}; C) as a function of time at different temperatures in air medium.

The plot of extent of conversion, α vs. time t obtained in air medium at four different temperatures for samples P_0, P_{50} and P_{100} is shown in Fig. 9A–C. These plots clearly show that the degree of conversion increases at high temperatures. Since the sample P_{50} is found to have high E_α value together with high thermal stability, it is expected to have increased time to failure. If a comparison is made at 550 °C (before reaching thermo-oxidation temperature) for these three samples, P_0 and P_{100} degrade faster than P_{50}. But, at high temperatures where the thermal-oxidation dominates (above 600 °C), P_{50} degrades faster than PEEK (sample P_0). More precisely, at 700 °C, the sample P_{50} degrades in <5 min while sample P_0 needs ca. 20 min to degrade (Fig. 9A and B). The above discussion clearly clarifies that the oxidation rate of PEEK gets enhanced upon PEI addition. These results are of use for a qualitative discussion of the thermal stability of PEEK/PEI blends. The optimized composition of PEEK/PEI blend (50/50) is in consistent with its optimized proportion reported [23,51].

Thus, the thermo-oxidation in PEEK and PEI gets initiated around the same temperature. But, the rate of thermo-oxidation in PEEK is slow. The introduction of PEI enhances the thermo-oxidation of PEEK. This enhancement in oxidation rate is an undesirable property and needs serious attention, particularly when this blend is used in aerospace applications. The use of suitable anti-oxidants could solve this problem.

4. Conclusions

For the first time, we have applied model-free kinetics to understand the thermal degradation of PEEK/PEI blends. The thermal degradation of PEEK/PEI blend involves two-step decomposition both in argon and air medium. The degradation mechanism of PEEK/PEI in air medium is different from that observed in argon. In argon medium, at the initial stages of conversion, the E_α value shows a slow increase and rises fast at the final stages of conversion. But, in air medium, E_α value gradually rises, peaks to a maximum and exhibits a near exponential decrease thereafter. The sample P_{50} shows maximum E_α value and also exhibits maximum thermal stability in air as well as in argon medium. However, the oxidation rate of PEEK gets enhanced upon PEI addition. The DSC results show a significant reduction in crystallinity for the sample P_{50}. Based on the combined model-free kinetics and DSC results, the PEEK/PEI (50/50) blend composition is suggested to have the optimum thermal stability.

Acknowledgement

The authors thank Director, DMSRDE for the encouragement and support during this work.

References

[1] O.B. Searle, R.H. Pfeiffer, Victrex poly(ethersulfone) and victrex poly(ether ether ketone) (PEEK), Polym. Eng. Sci. 25 (1985) 474–476.
[2] J.E. Harris, L.M. Robeson, Miscible blends of poly(aryl ether ketone)s and polyetherimides, J. Appl. Polym. Sci. 35 (1988) 1877–1891.
[3] M. Day, J.D. Cooney, D.M. Wiles, The thermal stability of poly(aryl ether ether ketone) as assessed by thermogravimetry, J. Appl. Polym. Sci. 38 (1989) 323–337.
[4] S.D. Hudson, D.D. Davis, A.J. Lovinger, Semicrystalline morphology of poly(aryl ether ether ketone)/poly(ether imide) blends, Macromolecules 25 (1992) 1759–1765.
[5] M. Shibata, Z. Fang, R. Yosomiya, Miscibility and crystallization behavior of poly(ether ether ketone ketone)/poly(ether imide) blends, J. Appl. Polym. Sci. 80 (2001) 769–775.
[6] G. Crevecoeur, G. Groeninckx, Binary blends of poly(ether ether ketone) and poly(ether imide). Miscibility, crystallization behavior and semicrystalline morphology, Macromolecules 24 (1991) 1190–1195.
[7] X. Kong, F. Teng, H. Tang, L. Dong, Z. Feng, Miscibility and crystallization behavior of poly(ether ether ketone)/polyimide blends, Polymer 37 (1996) 1751–1755.
[8] H.-L. Chen, R.S. Porter, Melting behavior of poly(ether ether ketone) in its blends with poly(ether imide), J. Polym. Sci. Part B Polym. Phys. 31 (1993) 1845–1850.
[9] B.S. Hsiao, B.B. Sauer, Glass transition, crystallization and morphology relationships in miscible poly(aryl ether ketones) and poly(ether imide) blends, J. Polym. Sci. Part B Polym. Phys. 31 (1993) 901–915.
[10] H.-L. Chen, R.S. Porter, Uniaxial draw of poly(ether ether ketone)/poly(ether imide) blends by solid-state coextrusion, Macromolecules 28 (1995) 3918–3924.
[11] M. Frigione, C. Naddeo, D. Acierno, Crystallization behavior and mechanical properties of poly(aryl ether ether ketone)/poly(ether imide) blends, Polym. Eng. Sci. 36 (1996) 2119–2128.
[12] A. Goodwin, R. Marsh, Dielectric and dynamic mechanical relaxation of poly(ether ether ketone)/poly(ether imide) blends below the glass transition, Macromol. Rapid Commun. 17 (1996) 475–480.
[13] J.F. Bristow, D.S. Kalika, Investigation of semicrystalline morphology in poly(ether ether ketone)/poly(ether imide) blends by dielectric relaxation spectroscopy, Polymer 38 (1997) 287–295.
[14] D.A. Ivanov, P.D.M. Lipnik, A.M. Jonas, Transmission electron microscopy studies on selectively stained poly(aryl ether ether ketone)/poly(ether imide) semicrystalline blends, J. Polym. Sci. Part B Polym. Phys. 35 (1997) 2565–2570.
[15] D.A. Ivanov, A.M. Jonas, Vitrification/devitrification phenomena during isothermal and non-isothermal crystallization of poly(aryl ether ether ketone) (PEEK) and PEEK/poly(ether imide) blends, J. Polym. Sci. Part B Polym. Phys. 36 (1998) 919–930.
[16] Y.S. Chun, H.S. Lee, H.C. Jung, W.N. Kim, Thermal properties of melt-blended poly(ether ether ketone) and poly(ether imide), J. Appl. Polym. Sci. 72 (1999) 733–739.
[17] A.M. Díez-Pascual, M. Naffakh, M.A. Gómez, C. Marco, G. Ellis, J.M. González-Domínguez, A. Ansón, M.T. Martínez, Y. Martínez-Rubi, B. Simard, B. Ashrafi, The influence of a compatibilizer on the thermal and dynamical properties of PEEK/carbon nanotube composites, Nanotechnology 20 (2009) 315707.
[18] C.E. Sroog, Polyimides, Prog. Polym. Sci. 16 (1991) 561–694.
[19] H.X. Nguyen, H. Ishida, Poly(aryl-ether-ether-ketone) and its advanced composites: a review, Polym. Compos. 8 (1987) 57–73.
[20] L.-H. Perng, Thermal decomposition characteristics of poly(ether imide) by TG/MS, J. Polym. Res. 7 (2000) 185–193.
[21] L. Abate, I. Blanco, A. Orestano, A. Pollicino, A. Recca, Evaluation of the influence of various (ether, ketone and sulfone) groups on the apparent activation energy values of polymer degradation, Polym. Degrad. Stab. 80 (2003) 333–338.
[22] R. Torrecillas, A. Baudry, J. Dufay, B. Mortaigne, Thermal degradation of high performance polymers—influence of structure on polyimide thermostability, Polym. Degrad. Stab. 54 (1996) 267–274.
[23] L. Torre, J.M. Kenny, Blends of semicrystalline and amorphous polymeric matrices for high performance composites, Polym. Compos. 13 (1992) 380–385.

[24] J. Kuljanin-Jakovljević, M. Marinović-Cincović, Z. Stojanović, A. Krklješ, N.D. Abazović, M.I. Čomor, Thermal degradation kinetics of polystyrene/cadmium sulfide composites, Polym. Degrad. Stab. 94 (2009) 891–897.
[25] M.E. Brown, M. Maciejewski, S. Vyazovkin, R. Nomen, J. Sempere, A. Burnham, J. Opfermann, R. Strey, H.L. Anderson, A. Kemmler, R. Keuleers, J. Janssens, H.O. Desseyn, C.-R. Li, T.B. Tang, B. Roduit, J. Malek, T. Mitsuhashi, Computational aspects of kinetic analysis. Part A. The ICTAC kinetics project-data, methods and results, Thermochim. Acta 355 (2000) 125–143.
[26] S. Vyazovkin, Advanced isoconversional method, J. Therm. Anal. 49 (1997) 1493–1499.
[27] S. Vyazovkin, C.A. Wight, Model-free and model fitting approaches to kinetic analysis of isothermal and non-isothermal data, Thermochim. Acta 340–341 (1999) 53–68.
[28] S. Vyazovkin, N. Sbirrazzuoli, Isoconversional kinetic analysis of thermally stimulated processes in polymers, Macromol. Rapid Commun. 27 (2006) 1515–1532.
[29] H. Polli, L.A.M. Pontes, A.S. Araujo, Application of model-free kinetics to the study of thermal degradation of polycarbonate, J. Therm. Anal. Calorim. 79 (2005) 383–387.
[30] D.M. Fernandes, A.A.W. Hechenleitner, E.A.G. Pineda, Kinetic study of the thermal decomposition of poly(vinyl alcohol)/kraft lignin derivative blends, Thermochim. Acta 441 (2006) 101–109.
[31] S. Vyazovkin, N. Sbirrazzouli, Mechanism and kinetics of epoxy-amine cure studied by differential scanning calorimetry, Macromolecules 29 (1996) 1867–1873.
[32] A.S. Araujo Jr., V.J. Fernandes, G.J.T. Fernandes, Thermogravimetric kinetics of polyethylene degradation over silicoaluminophosphate, Thermochim. Acta 392–393 (2002) 55–61.
[33] R. Ramani, J. Srivastava, S. Alam, Application of model-free kinetics to the thermal and thermo-oxidative degradation of poly(3-hexyl thiophene), Thermochim. Acta 499 (2010) 34–39.
[34] A.C.K. Chowlu, P.K. Reddy, A.K. Ghoshal, Pyrolytic decomposition and model-free kinetics analysis of mixture of polypropylene (PP) and low-density polyethylene (LDPE), Thermochim. Acta 485 (2009) 20–25.
[35] S. Vyazovkin, I. Dranca, X. Fan, R. Advincula, Degradation and relaxation kinetics of polystyrene-clay nanocomposite prepared by surface initiated polymerization, J. Phys. Chem. B 108 (2004) 11672–11679.
[36] S. Vyazovkin, I. Dranca, X. Fan, R. Advincula, Kinetics of the thermal and thermo-oxidative degradation of a polystyrene–clay nanocomposite, Macromol. Rapid Commun. 25 (2004) 498–503.
[37] M. Erceg, T. Kovačić, I. Klarić, Dynamic thermogravimetric degradation of poly(3-hydroxy butyrate)/aliphatic–aromatic copolyester blends, Polym. Degrad. Stab. 90 (2005) 86–94.
[38] D. Wu, Y. Zhang, M. Zhang, L. Wu, Morphology, nonisothermal crystallization behaviour, and kinetics of poly(phenylene sulfide)/polycarbonate blend, J. Appl. Polym. Sci. 105 (2007) 739–748.
[39] N.S. Vrandečić, B. Andričić, I. Klarić, T. Kovačić, Kinetics of isothermal thermo-oxidative degradation of poly(vinyl chloride)/chlorinated polyethylene blends, Polym. Degrad. Stab. 90 (2005) 455–460.
[40] B. Andričić, T. Kovačić, I. Klarić, Kinetic analysis of the thermo-oxidative degradation of poly(vinyl chloride) in poly(vinyl chloride)/methyl methacrylate-butadiene-styrene blends. 2. Nonisothermal degradation, Polym. Degrad. Stab. 79 (2003) 265–270.
[41] S. Jose, S. Thomas, P.K. Biju, P. Koshay, J. Karger-Kocsis, Thermal degradation and crystallization studies of reactively compatibilized polymer blends, Polym. Degrad. Stab. 93 (2008) 1176–1187.
[42] H.L. Friedman, Kinetics of thermal degradation of char-forming plastics from thermogravimetry. Application to a phenolic plastic, J. Polym. Sci. Part C Polym. Symp. 6 (1964) 183–195.
[43] T. Ozawa, A new method of analyzing thermogravimetric data, Bull. Chem. Soc. Jpn. 38 (1965) 1881–1886.
[44] J.H. Flynn, L.A. Wall, General treatment of the thermogravimetry of polymers, J. Res. Natl. Bur. Stand. Sect. A Phys. Chem. 70A (1966) 487–523.
[45] X.-G. Li, M.-R. Huang, Thermal decomposition kinetics of thermotropic poly(oxybenzoate-co-oxynapthoate) vectra copolyester, Polym. Degrad. Stab. 64 (1999) 81–90.
[46] L.H. Perng, C.J. Tsai, Y.C. Ling, Mechanism and kinetic modelling of PEEK pyrolysis by TG/MS, Polymer 40 (1999) 7321–7329.
[47] L.H. Perng, Thermal cracking characteristics of PEEK under different environments by the TG/FTIR technique, J. Polym. Sci. Part A Polym. Chem. 37 (1999) 4582–4590.
[48] Y.N. Gupta, A. Chakraborty, G.D. Pnadey, D.K. Setua, Thermal and thermo-oxidative degradation of engineering thermoplastics and life estimation, J. Appl. Polym. Sci. 92 (2004) 1737–1748.
[49] M. Naffakh, G. Ellis, M.A. Gómez, C. Marco, Thermal decomposition of technological polymer blends. 1. poly(aryl ether ether ketone) with a thermotropic liquid crystalline polymer, Polym. Degrad. Stab. 66 (1999) 405–413.
[50] H. Fujita, in: J. Crank, G.S. Park (Eds.), Diffusion in Polymers, Academic Press, New York, 1968.
[51] P.T. Rajagopalan, L.D. Kandpal, A.K. Tewary, R.P. Singh, K.N. Pandey, G.N. Mathur, Thermal behavior of polyetherimide PEEK blends, J. Therm. Anal. 49 (1997) 143–147.